PPPL-2318

PPPL-2318

UC20-A,D

(1) (25)

FUSION-NEUTRON PRODUCTION IN THE TFTR WITH DEUTERIUM NEUTRAL BEAM INJECTION

By

H.W. Hendel, A.C. England, D.L. Jassby,
A.A. Mirin, E.B. Nieschmidt

JUNE 1986

PLASMA
PHYSICS
LABORATORY

PRINCETON UNIVERSITY
PRINCETON, NEW JESEY

PREPARED FOR THE U.S. DEPARTMENT OF ENERGY,
UNDER CONTRACT DE-AC02-76-CHO-3073.

NOTICE

Printed in the United States of America

Available from:

National Technical Information Service
U.S. Department of Commerce
5285 Port Royal Road
Springfield, Virginia 22161

Price Printed Copy $ _____ ; Microfiche $4.50

*Pages	NTIS Selling Price
1-25	$7.00
25-50	$8.50
51-75	$10.00
76-100	$11.50
101-125	$13.00
126-150	$14.50
151-175	$16.00
176-200	$17.50
201-225	$19.00
226-250	$20.50
251-275	$22.00
276-300	$23.50
301-325	$25.00
326-350	$26.50
351-375	$28.00
376-400	$29.50
401-425	$31.00
426-450	$32.50
451-475	$34.00
476-500	$35.50
500-525	$37.00
526-550	$38.50
551-575	$40.00
567-600	$41.50

For documents over 600 pages, add $1.50 for each additional 25-page increment.

FUSION-NEUTRON PRODUCTION IN THE TFTR WITH DEUTERIUM NEUTRAL BEAM INJECTION

by

H.W. HENDEL[1], A.C. ENGLAND[2], D.L. JASSBY,
A.A. MIRIN[3], E.B. NIESCHMIDT[4]

PPPL--2318
DE86 013625

ABSTRACT

We report measurements of the fusion reaction rate in the Tokamak Fusion Test Reactor (TFTR) covering a wide range of plasma conditions and injected neutral beam powers up to 6.3 MW. The fusion-neutron production rate in beam-injected plasmas decreases slightly with increasing plasma density n_e, even though the energy confinement parameter $n_e\tau_E$ generally increases with density. The measurements indicate and Fokker-Planck simulations show that with increasing density the source of fusion neutrons evolves from mainly beam-beam and beam-target reactions at very low n_e to a combination of beam-target and thermonuclear reactions at high n_e. At a given plasma current, the reduction in neutron source strength at higher n_e is due to both a decrease in electron temperature and in beam-beam reaction rate. The Fokker-Planck simulations also show that at low n_e, plasma rotation can appreciably reduce the beam-target reaction rate for experiments with co-injection only. The variation of neutron source strength with plasma and beam parameters is as expected for beam-dominated regimes. However, the Fokker-Planck simulations systematically overestimate the measured source strength by a factor of 2 to 3; the source of this discrepancy has not yet been identified.

[1]On leave from RCA David Sarnoff Research Center, Princeton, NJ 08540
[2]On assignment from Oak Ridge National Lab., Oak Ridge, TN 37831
[3]National Magnetic Fusion Energy Computer Center, Lawrence Livermore National Lab., Livermore CA 94550
[4]On leave from Idaho Nat'l Engineering Lab., EG&G Idaho, Inc., Idaho Falls, ID 83415

1.0 INTRODUCTION

The Tokamak Fusion Test Reactor (TFTR) at Princeton University Plasma Physics Laboratory has been designed to study reactor-like plasmas near Q~1 (Q = fusion power/heating power), in neutral-beam-injected, two-energy component D-T plasmas, where the $n\tau_E$ (density x confinement time) requirement is less stringent than that for Maxwellian plasmas.[1] In this paper, the results of the initial fusion-neutron source strength and Q measurements for deuterium beams injected into deuterium plasmas are reported. In 1985 the TFTR[2] operated with neutral beam injection (NBI) power up to 6.3 MW in conjunction with ohmic heating, typically 0.5 - 2 MW, to obtain high plasma temperatures and neutron source strengths. The neutral beams were injected co-directional with the plasma current. The neutral beam particle energy E_b (nominally 80 keV) was about 2/3 of the eventual level (120 keV), and the beam power, P_b, about 1/5 of that expected to be available in 1987. Nevertheless, these initial low power experiments permit exploration of plasma regimes likely to be conducive to achieving power "breakeven" (Q ~ 1).

For a given capability of a tokamak and its neutral beams, there are basically three different approaches to generating high neutron source strength.[3]

1. <u>High electron density n_e and high $n_e\tau$.</u> Here thermonuclear reactions (rate = S_{tt}) among the Maxwellian target ions dominate, with beam-target fusion reactions playing a secondary role. This regime is potentially capable of Q>>1.

2. <u>Moderately high electron density n_e and moderately high $n_e\tau_E$.</u> Here the classical (i.e., Spitzer[4] fast-beam-ion slowing-down time, τ_s, is relatively short, so that the energetic-ion density n_h is relatively small, and most of the fusion-neutron production is due to beam-target reactions (rate = S_{bt}) and thermonuclear reactions. When S_{bt} is dominant, this regime is often called the TCT (two-component torus).[1]

3. <u>Low density and low $n_e\tau_E$.</u> Here τ_s is large, and n_h/n_e can exceed 0.2, so that a majority of the fusion reactions are due to reactions

between energetic ions (rate = S_{bb}); these reactions are called beam-beam self-reactions. The classical τ_s is several times longer than the electron energy confinement time, τ_{Ee}. Although the fusion reactivity drops rapidly with decreasing fast-ion energy, the fast ions must remain confined for several times τ_{Ee} to realize fully the potential neutron yield. When the neutral beams are both co- and counter-injected with roughly equal magnitude, this regime is often referred to as the CBT (colliding beam torus).[3]

The transition between the latter two regimes, as n_e is increased, is relatively abrupt, because $S_{bb} \propto n_h \cdot n_h \cdot \langle\sigma v\rangle_{bb} \propto \tau_s^2 \langle\sigma v\rangle_{bb} \propto (T_e^{2p}/n_e^2)\langle\sigma v\rangle_{bb}$, where the electron temperature T_e also tends to decrease with increasing n_e (see below). The parameter $p \simeq 3/2$ when the energetic ions slow down mainly on electrons: viz., at low T_e, or at high beam energy, or even at lower E_b when n_h exceeds the target-ion density. The parameter p becomes smaller as T_e/E_b increases. In the present range of beam energies, the initial beam ion slowing-down is slightly dominated by electron drag, considering that the bulk-ion density is significantly depleted by the energetic ions at lower n_e, where T_e is larger (because the total density is feedback controlled). Since most of the fusion reactions are produced by fast ions with energies not too far below the injection energy, p=3/2 tends to be a reasonable value to use in understanding the variation of S with plasma parameters, for both beam-target and beam-beam reactions. This remark applies to the full-energy component of a multispecies beam, which largely determines neutron source strength. Previous experiments on other tokamaks, notably PLT,[5] have provided indications of the existence of these different regimes of fusion-neutron production.

This paper describes experimental results from TFTR where the plasma and beam parameters span the latter two regimes defined above. Section 2 describes the experimental setup, Section 3 presents the measurements and their interpretation, and Section 4 discusses Fokker-Planck simulation of the beam-injected plasma. Extrapolation to higher beam power is discussed briefly in Section 5, and the Conclusions are given in Section 6.

2.0 TOKAMAK PARAMETERS AND NEUTRON DETECTORS

2.1 Plasma and Beam Parameters

Operation of the TFTR device and its plasma properties in the ohmic-heated regime as well as with neutral beam injection are described in Ref. 2. During the experiments discussed here, the plasma major and minor radii were approximately 2.55 and 0.82 m, respectively, the plasma current I_p ranged from 0.5 to 2.5 MA, and the toroidal magnetic field from 2.8 to 4.8 T. The ohmic heating power was usually 0.5 - 2 MW before injection.

The results described below were obtained with deuterium beam injection into both D and H plasmas. The NBI was co-directional with I_p for a pulse duration of 0.5 s, while the total plasma current duration was 3 to 3.5 s. Injection took place after the plasma had reached equilibrium. The nominal beam voltage of the 6 ion sources in the 2 injectors was 70-80 kV, but only about 50% of the power was at full voltage while 30% of the beam power was actually in half-voltage and 20% in one-third voltage particles. At low density, the co-directional NBI produced substantial plasma rotation (see below).

2.2 Neutron Detectors and Calibration

The neutron source strength was measured with a set of six fission detectors: two 1.3 g ^{235}U, two 1.3 g ^{238}U, one 18 g ^{235}U, and one 100 g ^{238}U chambers.[6] The 1.3 g ^{235}U detectors contained polyethylene moderators 5-cm thick, thermal neutron absorbers outside the moderator, and Pb gamma radiation shields 10-cm thick, resulting in a detection efficiency nearly independent of neutron energy. The ^{238}U detectors are sensitive only to neutrons above about 1 MeV energy and were covered by Pb shields only. Figure 1 shows the location of these detectors around the TFTR. Measurements using the multichannel collimator and the neutron energy spectrometer will not be discussed, but the instrumentation has been indicated for completeness.

In order to allow precise neutron source strength measurements, the ^{235}U fission detectors were calibrated <u>in situ</u> using D-D and D-T neutron generators and a ^{252}Cf neutron source inside the TFTR vacuum vessel.[7] Each calibration point source was moved through about 30 locations to simulate the volume occupied by the plasma, with all TFTR structures, diagnostics, and other

scatterers in place. Based on these results, the source strength measurements for plasma-produced neutrons are expected to have an error of $\lesssim$10%. The detectors were calibrated on 4 separate occasions over 2 years, which included periods of major reconfiguration in the TFTR Test Cell. The calibrations varied typically by ~10% for major changes in the scatterers, and by 1-2% when scattering conditions were similar. The total variance of all calibrations is about 10%. The calibration of the less sensitive three ^{238}U fission chambers was inferred from the ^{235}U chambers by cross calibration in regimes where count rates with good statistics overlap in both types of detectors.

In contrast to an ohmically heated plasma, the beam-target fusion reaction with NBI leads to anisotropic neutron emission.[8] The calibration was performed with both isotropic (^{252}Cf) and anisotropic (neutron generator) sources. The D-D neutron generator was rotated inside the TFTR vacuum vessel to determine the effect of the anisotropic differential cross section. The effect of the anisotropy was found to be negligible. This result is in agreement with: 1) calculations showing about 10% anisotropy when scattering is neglected[9] (for a worst case with the beam ion velocity parallel), and 2) the fact that in the detector location the total flux (including scattered neutrons as seen by the ^{235}U detectors) is calculated from a three-dimensional Monte Carlo model to be approximately 7 times the uncollided flux (as seen by the ^{235}U detectors).[10] For a more detailed discussion of the detectors and their calibration, and for neutron source strength results with ohmic heating and deuterium pellet injection, see Ref.11.

3.0 NEUTRON SOURCE STRENGTH MEASUREMENTS

3.1 Time Dependence of Neutron Source Strength

Here the neutron source strength S is defined as the instantaneous fusion-neutron production rate, in n/s. ($S = S_{bb} + S_{bt} + S_{tt}$.) Figure 2 shows the time dependence of S during a typical TFTR pulse with about 5 MW NBI operating for 0.5 s. When the beams are turned on, S increases rapidly and reaches its maximum value in about 0.1 s, where it remains until the beams are turned off. NBI increases S by one to three orders of magnitude above the value in the ohmic-heated (OH) regime, depending on the initial conditions. Immediately following turnoff of the NBI, S decays exponentially with a decay constant τ_n determined by the plasma parameters.

The plasma parameters used in the following subsections were derived from the raw data obtained by the TFTR plasma diagnostics and application of the SNAP code.[12]

3.2 Variation of S with Density and Plasma Current

The results discussed below (except those in Figs. 5 and 6) are based on TFTR discharges involving deuterium NBI into deuterium plasmas at approximately constant NBI power, $P_b \simeq 4.25 \pm 0.25$ MW. About 40 discharges were studied. Figure 3(a) shows S as a function of line-averaged electron density $\bar{n}_e$ for several values of I_p. In TFTR operation, large I_p is always associated with relatively high values of $\bar{n}_e$. For this beam power, the following experimental features are of interest:

(1) The highest values of S occur at low $\bar{n}_e$ (= 1-2 x 10^{19} m^{-3}), with the maximum value obtained at $I_p \simeq 1$ MA. For maximum values of S, the energy confinement time $\tau_E \simeq 0.1$ s, while τ_E can range up to 0.25 s at the higher $\bar{n}_e$ where S is slightly smaller.

(2) For $\bar{n}_e \lesssim 2.5 \times 10^{19}$ m^{-3}, S generally increases with I_p.

(3) At a given I_p, $S \propto 1/\bar{n}_e$ when I_p is small (Fig. 3(b)), but S is nearly independent of $\bar{n}_e$ at larger I_p, where $\bar{n}_e$ tends to be larger as well (Fig. 3(a)).

(4) S increases with T_e (at constant beam power) (Fig. 3(c)).

These features can be explained from the following facts:

(a) The beam-target reaction rate, $S_{bt} \propto n_h \cdot n_e \langle\sigma v\rangle_{bt} \propto (T_e)^p \langle\sigma v\rangle_{bt}$, is independent of $\bar{n}_e$ and dominates at moderate $\bar{n}_e$. At the highest $\bar{n}_e$ reached, S_{tt} is important but still less than S_{bt}. The slight reduction in T_e (for $I_p \simeq$ const) and decreased beam penetration with higher $\bar{n}_e$ may result in S_{bt} slowly dropping with $\bar{n}_e$.

(b) The energetic-ion self-reaction rate, $S_{bb} \propto n_h \cdot n_h \langle\sigma v\rangle_{bb} \propto (1/\bar{n}_e^2) T_e^{2p} \langle\sigma v\rangle_{bb}$, depends strongly on $\bar{n}_e$, and tends to dominate at low $\bar{n}_e$.

(c) Both beam-target and beam-beam reaction rates increase with T_e.

(d) Thomson scattering and electron cyclotron emission measurements show that T_e is highest (4-4.6 keV) at $I_p \simeq 1$ MA, where $\bar{n}_e$ is relatively low.

Increasing $\bar{n}_e$ tends to reduce the attainable T_e, even when I_p is increased (Fig. 4). S_{bt} also depends weakly on T_i because of the relative velocity of the beam and target ions, and also through the influence of this temperature on the energetic-ion velocity distribution. For the present set of experiments with co-injection only and $Z_{eff} > 1$, generally[3] $\langle\sigma v\rangle_{bb} \simeq \langle\sigma v\rangle_{bt}$. While $\langle\sigma v\rangle_{bt}$ can increase weakly when T_i is large, it is reduced significantly when the beams are solely co-injected and the plasma has a large rotational velocity because of the decrease in average relative velocity. Up to 6×10^5 m/s rotational velocity has been measured[13] in TFTR for $\bar{n}_e \simeq 10^{19} m^{-3}$ and $P_b \simeq 5$ MW. Large T_i or plasma rotation has essentially no effect on $\langle\sigma v\rangle_{bb}$.

Experimentally, NBI runs at low density with hydrogen target plasmas were found to give levels of S comparable to those achieved with deuterium plasmas, for the same plasma and beam parameters. This result is presumably due partly to the buildup of beam-injected deuterons in the thermal target plasma, and partly to the importance of beam-beam fusion reactions in low density plasmas. We also note that at low plasma densities up to 10% of the injected beam ions are not trapped by the plasma ("shinethrough" effect).

3.3 Variation of S with Electron Temperature

Optimal Current. Maximum S occurs at $I_p \simeq 1$ MA because of several effects. Higher values of I_p are concomitant with higher $\bar{n}_e$, resulting in smaller T_e. Increasing density also lowers S_{bb}. At values of $I_p < 1$ MA, T_e and T_i are degraded by reduction in τ_E, and calculations indicate shorter lifetime of energetic ions. Also, $T_e(0)$ increases fairly strongly with I_p up to $\simeq 1$ MA, but only weakly at higher currents.

The strong density dependence of S at lower I_p is due in part to the slow reduction in T_e with increasing $\bar{n}_e$ in this range (see Fig. 4). Nevertheless, most of the reduction in S is probably due to the increase in density itself, which strongly reduces the beam-beam reaction rate, as noted above. The weak density dependence of S at higher I_p indicates the dominance of beam-target reactions in the corresponding density range. Thus it appears that at $\bar{n}_e \leq 2.5 \times 10^{19} m^{-3}$ ($I_p \leq 1$ MA), both beam-beam and beam-target reactions are important, while for $\bar{n}_e \geq 3 \times 10^{19} m^{-3}$ ($I_p > 1$ MA), beam-target reactions become increasingly dominant, for the NBI power used. We note that for the conditions of this paper, thermonuclear reactions are never dominant.

For all discharges with $I_p \leq 1$ MA, the calculated $\tau_s/\tau_{Ee} > 3$, which is also a characteristic feature of the energetic-ion (CBT) regime.[3] To realize the full potential neutron production, the fast ion confinement time must exceed τ_s. The higher $\bar{n}_e$ associated with higher I_p decreases τ_s while higher I_p increases τ_{Ee}, so that τ_s/τ_{Ee} quickly approaches 1, which is typical of the TCT regime.

3.4 Variation of S and Q with Beam Power

The fusion energy amplification for deuterium plasmas is defined as

$$Q = \frac{\text{fusion power}}{\text{beam power + ohmic power}} = \frac{S \times 7.3 \times 1.6 \times 10^{-19}}{P_b + P_{oh}}, \qquad (1)$$

where the powers are in MW, and 7.3 MeV is the total energy released in both branches of the D-D reaction. (The branches have approximately the same cross sections.) This equation neglects contributions from burnup of the T and ^3He reaction products and assumes steady-state conditions.

Figure 5 shows measured and calculated (FPT code) S and Q versus injected beam power P_b at $I_p = 2.2$ MA, where $\bar{n}_e \simeq 4.5 \times 10^{19} m^{-3}$. The calculations of S and possible reasons for the overestimate are discussed below. Figure 6 shows the same experimental results plotted against ($P_b + P_{oh}$), as well as the variation of P_{oh}, $T_e^{3/2}$, and $\bar{n}_e$ with input power. Note that $\bar{n}_e$ is essentially constant for this beam power scan.[14] At the high density and relatively low ion temperature that characterize this set of data, beam-target reactions are dominant.

Upon the application of 1 MW of beam power, S increases by a factor of 7 and Q by a factor of 5. The neutron source strength S increases approximately proportionally to further increases in P_b, with Q rising only slowly. The increase in Q in going from $P_b \simeq 1$ MW to $P_b \simeq 5.5$ MW is a factor of about 1.6 [see Fig. 6(b)]. Thus higher T_e will have to be achieved to realize higher Q.

Most of the results presented in this paper are for $P_b \simeq 4.25$ MW. However, with $P_b = 5.7$ MW, the highest neutron source strength ($\sim 4 \times 10^{14}$/s) was achieved so far at $\bar{n}_e = 1.9 \times 10^{19} m^{-3}$ and 1.2 MA plasma current. The corresponding Q is about 9×10^{-5}. Using the known D-T/D-D cross-section and reaction energy ratios, the equivalent Q in D-T operation, for the same beam and plasma conditions, would be 0.04 to 0.06, depending on the fraction of reactions that are beam-target. This calculation assumes a 100% T target plasma.

Variation with Confinement Time. Figure 7 shows S versus τ_E as determined from the SNAP analysis.[12] Even at a single I_p, there is no clear dependence of S on τ_E. The neutron source strength is evidently not a direct function of τ_E. In fact, S (or Q) depends primarily on T_e (and on $\bar{n}_e$ for S_{bb}), for which τ_E can have a range of values depending on $\bar{n}_e$, P_b, and I_p. This characteristic is typical of neutron production dominated by beam-target and beam-beam self-reactions.[1],[3]

3.5 Neutron Source Decay Time

The e-folding time for decay of S after beam turnoff has been measured for the set of discharges with $P_b \simeq 4.25$ MW. For the beam-target regime, where Coulomb interactions among the energetic ions can be ignored, the decay time τ_n is given by[5]

$$\tau_n = \frac{\tau_{se}}{3} \ln \frac{E_b^{3/2} + E_c^{3/2}}{E_n^{3/2} + E_c^{3/2}} \qquad (2)$$

where τ_{se} is the slowing-down time on electrons alone, E_n is the energy at which the fusion cross-section is reduced by 1/e from the value at the injection energy, E_b, and E_c is the critical energy at which the electron and bulk-ion contributions to the slowing-down rate are approximately equal ($E_c \simeq$

18.5 T_e for $D^0 + D^+$ when $n_h/n_a \simeq 0$). Equation (2) has the limitations that (i) it applies only to a single beam-energy constituent, (ii) it neglects depletion of the energetic-ion population by charge exchange or other processes, (iii) it neglects bulk-plasma rotation,[13] (iv) it neglects depletion of the bulk-ion population by the energetic ions, and (v) it includes only beam-target reactions. The plasma rotation causes a small enhancement of the slowing-down rate when bulk-ion drag is important. We also note that τ_n is calculated using values of T_e and $\bar{n}_e$ measured before beam turnoff, so that subsequent changes of these parameters during the neutron source decay are neglected. These changes are relatively small.

Figure 8 shows the relation between the predicted (for central values of n_e and T_e) and observed values of τ_n. The measured values are generally less than the predicted values, with the deviation tending to increase at larger τ_n. The discrepancy may be due to the effects mentioned above, all of which (except iv) serve to reduce τ_n. However, an independent and more sophisticated calculation of τ_n using the FPT Fokker-Planck code (see Sec. 4.0) predicts values comparable (±25%) to those from Eq. (2). The reasonable correlation over the entire range indicates that the fast-ion slowing-down process has essentially the classical variations with T_e and $\bar{n}_e$. Nevertheless, the possibility of an enhanced thermalization rate or of enhanced radial diffusion of fast ions cannot be excluded. (See Sec. 4.4).

Figure 9 shows the relation between S and calculated τ_s at I_p = 0.8 MA. As expected, S increases with τ_s. Calculations show that $\tau_n \simeq \tau_s/5$ for this data set, reflecting the fact that most of the neutron production is due to fast ions with energies fairly close to the injection energy. Thus for the full-energy beam component, for which $E_b \geq E_c$, electron drag is approximately equal to ion drag in the energy range responsible for most of the fusion reactions. For conditions of co-injection and strong plasma rotation, with $Z_{eff} \simeq 1$, ion drag may dominate.

4.0 FOKKER-PLANCK SIMULATION

4.1 The FPT Code

The National Magnetic Fusion Energy Computer Center's FPT (Fokker-Planck/Transport) code[15] was used to simulate neutral beam injection in the TFTR at low to moderate density. The full FPT code utilizes a numerical one-dimensional transport model coupled with a fully nonlinear two-dimensional Fokker-Planck analysis of beam-injected energetic ions at each plasma radius. This code has been applied before to simulation of beam-injected plasmas in the PLT device and other tokamaks.[5],[16] In the present simulation the transport mechanisms are turned off, and the measured profiles of n_e and T_e and an estimated one for T_i are specified and a neutral density is assumed. Impurity ions are assumed to have $Z = 26$ and 7, with Z_{eff} independent of radius. The nominally deuterium target plasma also contains approximately 15% hydrogen. The velocity distributions of the energetic ions are iterated to steady-state values using the experimental plasma parameters and profiles.

The treatment includes a self-consistent beam-deposition code, which includes trapping by charge exchange and ion impact collision of the fast neutrals on electrons, Maxwellian warm ions and non-Maxwellian energetic ions. Orbit losses of newly ionized energetic ions and subsequent charge-exchange losses and recapture are taken into account. The most important assumption in the Fokker-Planck equation is that the injected energetic ions diffuse in velocity-space and thermalize classically, with no spatial diffusion. An energetic ion is removed from the fast-ion distribution when it decelerates to an energy $E_c = 3/2 \cdot T_e$. The fusion reaction cross sections used are from a fit by Futch et al.[17] for the FPT code and from a fit by Miley et al.[18] for the SNAP calculations.

4.2 Calculated Sources of Fusion Neutrons

There is considerable uncertainty concerning Z_{eff} in the central plasma region and the radial profile of impurity concentration. For the low $\bar{n}_e$-low current conditions studied in Table 1, measurements[19],[20] indicate that $Z_{eff} \geq 2.0$. Table I gives the results of FPT calculations for different values of Z_{eff} (here assumed to be independent of radius). It turns out that

for purely co-injected beams, as in the present experiments, the predicted S is only weakly dependent on Z_{eff}. When $Z_{eff} = 1$, there is little pitch-angle scattering of the energetic ions, and only 11% of S is due to beam-beam reactions (rate $\propto S_{bb}$). When Z_{eff} increases, S_{bt} is reduced by impurity dilution of the target-ion population. (The decrease in n_h/n_e is due to the electrons that neutralize the impurity ions.) On the other hand, at $Z_{eff} = 4$, pitch-angle scattering of the energetic ions is enhanced, thereby increasing $\langle\sigma v\rangle_{bb}$ so that S_{bb} accounts for 44% of the total reaction rate. The increase in S_{bb} compensates for the decrease in S_{bt}.

In both cases, n_h/n_e in the plasma center is calculated to be close to 0.6, although when averaged over the plasma volume, $\langle n_h/n_e\rangle \simeq 0.17$. The results in Table I also show that if one of the two beams were to be counter-injected rather than co-injected, the neutron source strength would be even higher, the exact amount depending on Z_{eff}. This increase comes from the greatly enhanced beam-beam reactivity $\langle\sigma v\rangle_{bb}$ in the CBT mode,[3] as well as the elimination of plasma rotation by the balanced beam injection. These effects have important influence on S only at low plasma density. The higher S values expected from balanced injection for beam-beam reactions would also be much less pronounced in future D-T experiments with $E_b = 120$ keV, due to the D-T reactivity maximum at about 125 keV relative energy.

Additional FPT analyses indicate that a relatively small increase in density (a factor $\simeq 1.5$) causes the plasma to switch over to a regime where n_h/n_e at $r = 0$ is reduced to about 0.2. In this case more than half the fusion reactivity comes from beam-target reactions and most of the rest from thermonuclear reactions.

4.3 Effect of Bulk-Plasma Rotation

The results shown in Table II were calculated using experimental conditions for low density TFTR shots that gave approximately 3.3×10^{14} n/s for D + D. The warm ions are represented as displaced Maxwellians, with the rotation speed assumed to be parabolic in radius in approximate agreement with previous observations.[21] Evidently, the large plasma rotation observed at low $\bar{n}_e$ is found to cause a significant reduction in the calculated beam-target reaction rate. The beam-target source strength drops by 54% with rotation when $Z_{eff} = 1.0$, by 49% when $Z_{eff} = 1.5$ and by 35% when $Z_{eff} = 4$. In the

latter cases pitch-angle scattering of the hot (beam-injected) ions is enhanced, so that velocity displacement of the warm ions has much less effect on the average relative velocity of the hot and warm ions.

In the results shown in Table II, bulk ion rotation was included both in calculating the beam-target reactivity $\langle\sigma v\rangle_{bt}$ and in the Fokker-Planck operator. Rotation of the bulk plasma causes the co-injected fast ions to thermalize more quickly, because of the reduced relative velocity with the thermal ions. However, the dominant effect on S resulting from plasma rotation is due to the change in the beam-target reactivity.

4.4 Discrepancy Between Simulation and Experimental Results

For the cases calculated with the FPT code in Fig. 5 and the Tables and for the cases calculated with the SNAP code, the simulated neutron source strengths are a factor of the order of 2-3 higher than the measured values. Possible reasons for this discrepancy are the following:

(1) The neutron detectors may be miscalibrated. However, in view of the care taken and of the many calibrations performed, the systematic error in S is probably less than 10%.[7,11]
We note that Indium-foil neutron activation measurements of the neutron source strength S confirmed the S measurements obtained based on fission detectors. The activation method, however, has a larger error (± 30%), since it could not be directly in-situ calibrated, so that the scattered neutron flux had to be taken from calculations.[10]
For completeness, we also note that for ohmically heated plasmas (without NBI) the ion temperatures obtained from the Titanium Kα Doppler-broadening measurements are in agreement with the T_i measurements from the neutron source strengths in about 30% of all discharges.[22] For the rest of the discharges up to 15% higher T_i values are obtained by the Titanium Kα measurements. (The errors are expected to be: ΔT_i(Kα)±5%; neutron source strength ΔT_i(N)±8%). Calculating a neutron yield from the higher Titanium Kα T_i values (using an assumed radial T_i profile) leads to calculated S values up to two times higher than those measured. For the charge

exchange T_i measurements, when an opacity correction is applied to the passive charge-exchange data, a similar agreement (±15%) with neutron and K_α temperatures is obtained.[23]

(2) The energetic ions may diffuse outward while thermalizing. However, this diffusion rate would have to be exceptionally large, because FPT code analysis showed that S would be reduced by no more than 5% for a hot-ion diffusion rate $1/\tau_p \simeq 1/\tau_{Ee}$. Recent observations on TFR[24] indicate that the fast-ion deposition profile may expand almost immediately after injection. That effect, if present in the TFTR, would lead to a reduction in S and Q because the typical fast ion would slow down in a region of lower T_e.

(3) Instabilities may enhance the energetic-ion thermalization rate above the classical values. While there is no clear evidence for such an enhancement from charge-exchange neutral spectra,[25] the comparison of measured and calculated neutron decay times after NBI turn-off (Fig. 8) may indicate somewhat enhanced thermalization rates.

(4) The electron temperature used in the simulation is derived from Thomson scattering data, and may be in error by ±5 to 10%. Such a correction would change the calculated S by ±10-15%.

(5) The ion temperature used in the simulation may be too large, and the T_i profile (which is not measured) may be too broad. An error here would be important only at higher density ($\bar{n}_e \gtrsim 5 \times 10^{19} m^{-3}$), where thermal reactions are significant.

(6) The neutral density used in the simulation may be substantially higher than inferred from experimental data. The maximum reduction calculated in S by increasing the neutral density to the largest conceivable value ($3 \times 10^{13} m^{-3}$ in the plasma center, as obtained from neutral particle diffusion codes) is less than 20%.

(7) Neutral beam penetration may be reduced by the recently described multistep collision process.[26] This effect is small when $E_b \simeq 80$ keV and $\bar{n}_e = 3 \times 10^{19} m^{-3}$, but may be of some importance at higher $\bar{n}_e$ (and E_b).

(8) The fusion reaction rate for NBI is due mainly to the full-energy beam component. The uncertainty of approximately 20% for the assumed full-energy fraction[27] results in an uncertainty of the calculated neutron source strength of ±20%.

(9) The fusion reaction cross section fits used in our analysis[17] may contain errors. A comparison of two widely used fits[17],[18] shows that of Ref. 17 60% above that of Ref. 18 at 10 keV (ohmic heating regime) and 5% below at 100 keV (NBI regime), and smaller differences at intermediate energies.

(10) The effect of dilution of the deuterium plasma by hydrogen and impurities may be greater than assumed. The hydrogen fraction was measured by comparison of the D_α and H_α lines and by a residual gas analyzer, neither of which determines the central dilution of the deuterium directly. The impurities were measured by visible bremsstrahlung and by soft x-ray analysis, both of which are weighted more toward the plasma center.

(11) The effects of errors in the density profile are probably small in comparison to the effects of errors in the temperature profile.

All these potential sources of error taken together could result in about a factor of 2-3 overprediction of neutron source strength, if the uncertainties all acted in the same direction. It is still possible that there is some additional significant effect not yet included in the simulation.

5.0 EXTRAPOLATION TO HIGHER BEAM POWER AND ENERGY

Higher Q. The planned increase in beam voltage to 120 kV, concomitant with greatly improved beam species composition, is expected to increase Q by a factor of about 3 based on the energy dependence of $\langle\sigma v\rangle_{bt}$ and τ_s, for the same bulk-plasma parameters. Of the four beam injectors now installed, one is oriented for counter-injection; the increase in energetic-ion reactions at low density should lead to another factor of at least 1.5 increase in S_{bb}, for the same beam power and bulk-plasma conditions. Thus overall Q will increase by a factor of approximately 5, reaching about 5×10^{-4} in deuterium only.

In order to realize still higher Q, it is necessary that T_e and T_i increase with beam power. If T_e and T_i remain constant, S_{bt} and S_{tt} would not change. However, since $S_{bb} \propto n_h^2 \propto P_b^2/n_e^2$, Q would increase even at constant T_e, if n_e were to increase more slowly than P_b. For S_{bt} and S_{bb}, the more important temperature is T_e. In the 1985 TFTR experiments, the plasma exhibited only a modest increase of T_e with P_b (Fig. ..), apparently due mainly to the decrease in τ_{Ee} with P_b, but also partly due to the reduction of ohmic heating in the low density regime with intense beam injection. The latter effect will become an insignificant factor when P_b is very large, and other experiments in TFTR and in Doublet III[28] suggest that τ_{Ee} may not decrease indefinitely with increasing P_b. In that case there are good prospects for appreciably increasing T_e in high-powered experiments. Results obtained in 1986 after this paper was submitted for publication indicate that at higher P_b than available in 1985, the electron temperature increases further, resulting in increased Q.

Beam-Beam vs Beam-Target Reactions. The importance of beam-beam reactions at low density can be seen from: (1) S decreases significantly with increasing density (even after accounting for the small decrease in T_e with increasing density); (2) FPT code and other simulations show that $n_h \simeq n_e$ for $r \lesssim 30$ cm; (3) hydrogen target plasmas give nearly the same S as deuterium target plasmas; (4) ^{3}He gas-puffing experiments[29] show that, after beam turnoff, the decay time of proton source strength intensity from the D-^{3}He beam-target reaction is comparable with the decay time of neutron source strength intensity from D-D reactions; this relation is expected when beam-beam reactions are dominant.

The experiments suggest and Fokker-Planck simulations show that only a relatively small increase (factor ~ 1.5) in plasma density is required to switch the principal source of fusion-neutron production from beam-beam and beam-target reactions, to beam-target and thermonuclear reactions, with relatively small changes in Q at the transition. Further simulations indicate that this feature will persist as the injected power is raised to the 30 MW level, and E_b increases to 120 keV with improved beam species composition. Thus the choice of operating regime may depend on the level of τ_{Ee} that can be attained, and in the case of D-T operation, whether tritium beams are available. For the present beam and plasma conditions, deuterium pellet injection,[20] although increasing the neutron source strength S during ohmic heating, does not improve S with NBI. The concomitant reduction of T_e reduces both beam-beam and beam-target reaction rates and the increase of n_e decreases the beam-beam reaction rates. However, the Maxwellian reaction rates during NBI are increased with pellet injection, as indicated by the fact that S remains at higher than pre-beam levels after beam turnoff. For higher T_i, when Maxwellian reactions are dominant, the effect of pellet injection may thus be expected to increase the neutron source strength.

6.0 CONCLUSIONS

Initial deuterium neutral beam injection into D and H plasmas in the TFTR shows that, for the present beam power, maximum neutron source strength ($S \simeq 4\times10^{14}$n/s) and fusion gain Q (8×10^{-5} in $D^0 \rightarrow D^+$) are achieved at moderate plasma current (~ 1 MA) and low density $\bar{n}_e$ = 1-2 x $10^{19}m^{-3}$. In this regime the plasma confinement quality factor $\bar{n}_e\tau_E$ is much less than at high density, and Fokker-Planck simulations show that both beam-beam and beam-target reactions are important. With increasing density, beam-beam reactions become unimportant as indicated by the experiments and simulations, while beam-target reactions dominate and thermonuclear reactions eventually become significant. The attainable Q is reduced somewhat at the largest density, mainly because of smaller T_e but also because of the absence of beam-beam reactions and reduced beam penetration.

The reduction in Q with increasing $\bar{n}_e$ occurs even though higher density necessitates operating at higher current where τ_E is larger. In fact the data exhibit no particular dependence of S or Q on τ_E. The results show that S and

Q depend primarily on T_e, a characteristic expected of fusion-neutron production dominated by beam-target and energetic-ion self-reactions. In Maxwellian plasmas, by contrast, Q will be determined principally by T_i and $\bar{n}_e\tau_E$. In addition to improved beam parameters, substantially larger $T_e(0)$ will be required for Q to approach 1 in D-T operation.

The behavior of the measured neutron source strength with plasma and beam parameters is semi-quantitatively understood; that is, the scaling of S and Q with these parameters is as expected for beam-dominated regimes. However, the Fokker-Planck simulations systematically overestimate the measured source strength by a factor of the order of 2-3. While numerous sources of uncertainty exist, precisely which of these are responsible for the discrepancy has not yet been identified.

ACKNOWLEDGEMENTS

It is our pleasure to acknowledge the many engineers, physicists, programmers, and technicians whose dedication to the TFTR program has made this work possible. We acknowledge especially helpful discussions with Drs. M. Bitter, R.A. Ellis, Jr., R.J. Goldston, L.R. Grisham, R.J. Hawryluk, W.W. Heidbrink, K.W. Hill, D.L. Hillis, D.M. Meade, J.D. Strachan, G. Taylor, R. Yoshino, K.M. Young, M.C. Zarnstorff, and S.J Zweben. This work was supported by U.S. Department of Energy Contract No. DE-AC02-76CH03073. One of the authors (A.C. England) was supported by the Office of Fusion Energy, U.S. Department of Energy Contract No. DE-AC05-84OR21400 with Martin Marietta Energy Systems, Inc.

REFERENCES

1. J.M. Dawson, H.P. Furth, and F.H. Tenney, Phys. Rev. Lett. 26, 1156 (1971).

2. P.C. Efthimion, et al., Phys. Rev. Lett. 52, 1492 (1984) (Ohmic heating results). K.M. Young, et al., Plasma Phys., 26, 11 (1984). M. Murakami, et al., Fusion Technology 8, Part 2A, 657 (1985) (NBI results).

3. D.L. Jassby, Nucl. Fusion 17, 305 (1977).

4. L. Spitzer, Jr., Physics of Fully Ionized Gases, 2nd Ed. (John Wiley & Sons, Inc., 1962), p. 134.

5. J.D. Strachan, et al., Nucl. Fusion 21, 67 (1981).

6. H.W. Hendel, K. Matsuoka, and L.E. Samuelson, Proc. Fourth ASTM-Euratom Symp. on Reactor Dosimetry (Nat. Bureau of Standards, Washington, DC, 1982), CONF-820321/V2, p. 94.

7. E.B. Nieschmidt, et al., Rev. Sci. Instr. 56, 1084 (1985).

8. N. Jarmie and R.E. Brown, Nucl. Inst. and Methods B10/11, 405 (1985).

9. W.W. Heidbrink, private communication.

10. L.P. Ku, J.A. Kolibal, and S.L. Liew, Princeton Plasma Physics Laboratory Report No. PPPL-2244 (1985). Note that ~50% of the neutrons in the source energy group are scattered neutrons (Private communication with L.P. Ku).

11. H.W. Hendel, IEEE Transact. NS 33, 670 (1986).

12. H.H. Towner, et al., Bull. Am. Phys. Soc. 28, 1252 (1983).

13. M. Bitter et al., Phys. Rev. A. 32, 3011 (1985).

14. M. Murakami, et al., presented at 12th European Conference on Controlled Fusion and Plasma Physics, Budapest, Hungary (1985), Plasma Physics and Controlled Fusion, Vol. 28, 1A, p. 17 (1986).

15. J. Killeen, A.A. Mirin, and M.G. McCoy, Modern Plasma Physics (IAEA, Vienna, 1981), p. 395.

16. A.A. Mirin, D.L. Jassby, IEEE Trans. Plasma Science PS-8, 503 (1980); R.D. Gill, G.D. Kerbel, and A.A. Mirin, Plasma Physics & Contr. Fusion 26 1B, 341 (1984).

17. A.H. Futch, Jr., J.P. Holdren, J. Killeen, and A.A. Mirin, Plasma Physics 14, 211 (1972). (This fit is due to earlier unpublished work by A.Winslow, 1958, L.L.N.L. Recent work by G.M. Hale, LASL, gives additional credence to Winslow's fit. See Ref. 8.)

18. G.H. Miley, H. Towner, and N. Ivich, University of Illinois, C-U Campus, Report COO-2218-17 (1974). (This fit is due to earlier work by D.H. Duane, see BNWL-1685, 1972.)

19. P.C. Efthimion, et al., presented at 10th Intl. Conf., London, 1984, Plasma Physics and Controlled Nuclear Fusion Research 1984 (IAEA, Vienna, 1985), Vol. I, p. 29. (Note that NBI does affect Z_{eff} negligibly when $\bar{n}_e$ is allowed to rise due to the NBI: Private Communication with K.W. Hill.)

20. G.L. Schmidt, et al., Proceedings of 12th European Conference on Controlled Fusion and Plasma Physics (Budapest, Hungary, 1985), Vol. 2, p. 674.

21. K. Brau, et al., Nucl. Fusion 23, 1643 (1983).

22. K.W. Hill, et al., Rev. Sci. Instr. 56, 1165 (1985).

23. S.S. Medley, et al., Proceedings of 12th European Conference on Controlled Fusion and Plasma Physics (Budapest, Hungary, 1985), Vol. 1, p. 343.

24. Equipe TFR, presented by M. Fois, in Proceedings of 13th Conference on Controlled Fusion and Plasma Heating (Schliersee, West Germany, 1986).

25. R. Kaita, et al., Princeton Plasma Physics Report No. PPPL-2321 (1986).

26. C.D. Boley, R.K. Janev, and D.E. Post, Phys. Rev. Lett. 52, 534 (1984).

27. L.R. Grisham, private communication.

28. H.K. Burrell, et al., presented at 10th International Conference, London (1984), Plasma Physics and Controlled Nuclear Fusion Research 1984 (IAEA, Vienna, 1985), Vol. I, p. 131.

29. D.L. Hillis, et al., Bull. Am. Phys. Soc. 30, 1521 (1985); A. Chan, and J.D. Strachan, Bull. Am. Phys. Soc. 30, 1522 (1985).

TABLE I

FPT CODE CALCULATION OF SOURCES OF FUSION NEUTRONS AT LOW DENSITY

Experimental Conditions

Co-injection only	P_b = 4.8 MW
$T_e(0)$ = 4.2 keV	$n_e(0) = 2.2 \times 10^{19} m^{-3}$
I_p = 0.8 MA	Measured S = 3.3×10^{14} n/s

Results of FPT Calculations

Injector Orientation	Z_{eff}	n_h/n_e at r=0	$\langle n_h/n_e \rangle$	TOTAL S 10^{14}/s	% Distribution of Reactions BEAM-BEAM	BEAM-TARGET	THERMAL IONS
Co-injectn. only	1.0	0.62	0.17	7.7	12	74	14
"	1.5	0.61	0.17	7.2	20	68	12
"	4	0.49	0.16	5.6	44	51	5
1 Co-inj. & 1 ctr-inj.	1.0	0.64	0.17	11.4	41	49	10
"	1.5	0.58	0.16	9.9	43	48	9
"	4	0.47	0.16	6.8	54	41	5

TABLE II.

FPT CODE CALCULATION OF EFFECT OF BULK-PLASMA ROTATION ON NEUTRON SOURCE STRENGTH

Experimental Conditions

Co-Injection only	P_b = 4.8 MW
$T_e(0)$ = 4.2 keV	$n_e(0) = 2.2 \times 10^{19} m^{-3}$
I_p = 0.8 MA	Measured S = 3.3×10^{14} n/s

Results of FPT Calculation

Z_{eff}	CENTRAL ROTATION (keV)	NEUTRON SOURCE STRENGTH (10^{14} n/s) TOTAL S	BEAM-BEAM	BEAM-TARGET	THERMAL IONS
1.0	0.0	7.7	1.0	5.7	1.0
1.0	5.0	4.3	0.6	2.6	1.1
1.5	0.0	7.2	1.5	4.9	0.9
1.5	5.0	4.5	1.1	2.5	0.9
4.0	0.0	5.6	2.4	2.9	0.3
4.0	5.0	4.5	2.3	1.9	0.3

Note: A rotation of 5.0 keV corresponds to 7×10^5 m/s, for deuterons.

FIGURE CAPTIONS

FIG. 1 Plan view of neutron detectors around TFTR.

FIG. 2 Time evolution of neutron source strength for $D^0 + D^+$, at $\bar{n}_e \simeq 2.5 \times 10^{19} m^{-3}$, $I_p = 0.8$ MA, and $P_b = 3.7$ MW.

FIG. 3 Measured neutron source strength vs. line-averaged electron density and central electron temperature, for $E_b \simeq 75$ keV and $P_b \simeq 4.25$ MW. The lines are linear regression fits, which include all three current values in 3(c). The time of the measurement in this and all following figures is that of the Thomson scattering measurement, which is generally near turnoff of the neutral beams.

FIG. 4 Central electron temperature vs. line-averaged electron density. $P_b \simeq 4.25$ MW. $I_p = 1.0$, 1.4, 1.8, and 2.2 MA.

FIG. 5 (a) Neutron source strength and (b) Q vs. beam power for $I_p = 2.2$ MA. (Same conditions as Fig. 6).

FIG. 6 (a) Neutron source strength, (b) Q, (c) $T_e^{3/2}$, and (d) line-averaged electron density vs. total input power, at $I_p = 2.2$ MA. The variation of ohmic power with total input power is shown in (b).

FIG. 7 Neutron source strength vs. bulk-plasma energy confinement time, for all data at $P_b \simeq 4.25$ MW.

FIG. 8 Measured vs. predicted decay time of neutron intensity after beam turnoff, for $P_b \simeq 4.25$ MW.

FIG. 9 Measured source strength vs. fast-ion slowing-down time calculated from plasma parameters for $P_b \simeq 4.25$ MW. A linear dependence is expected.

#85X2069

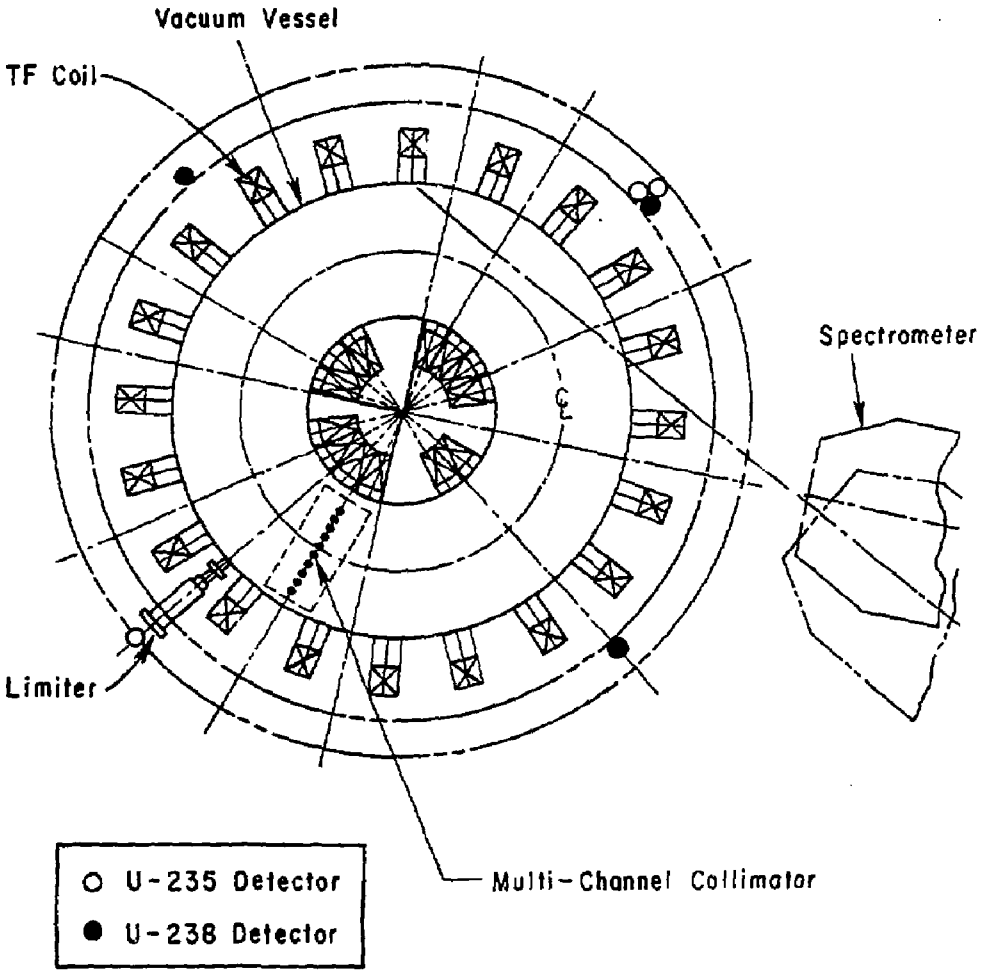

Fig. 1

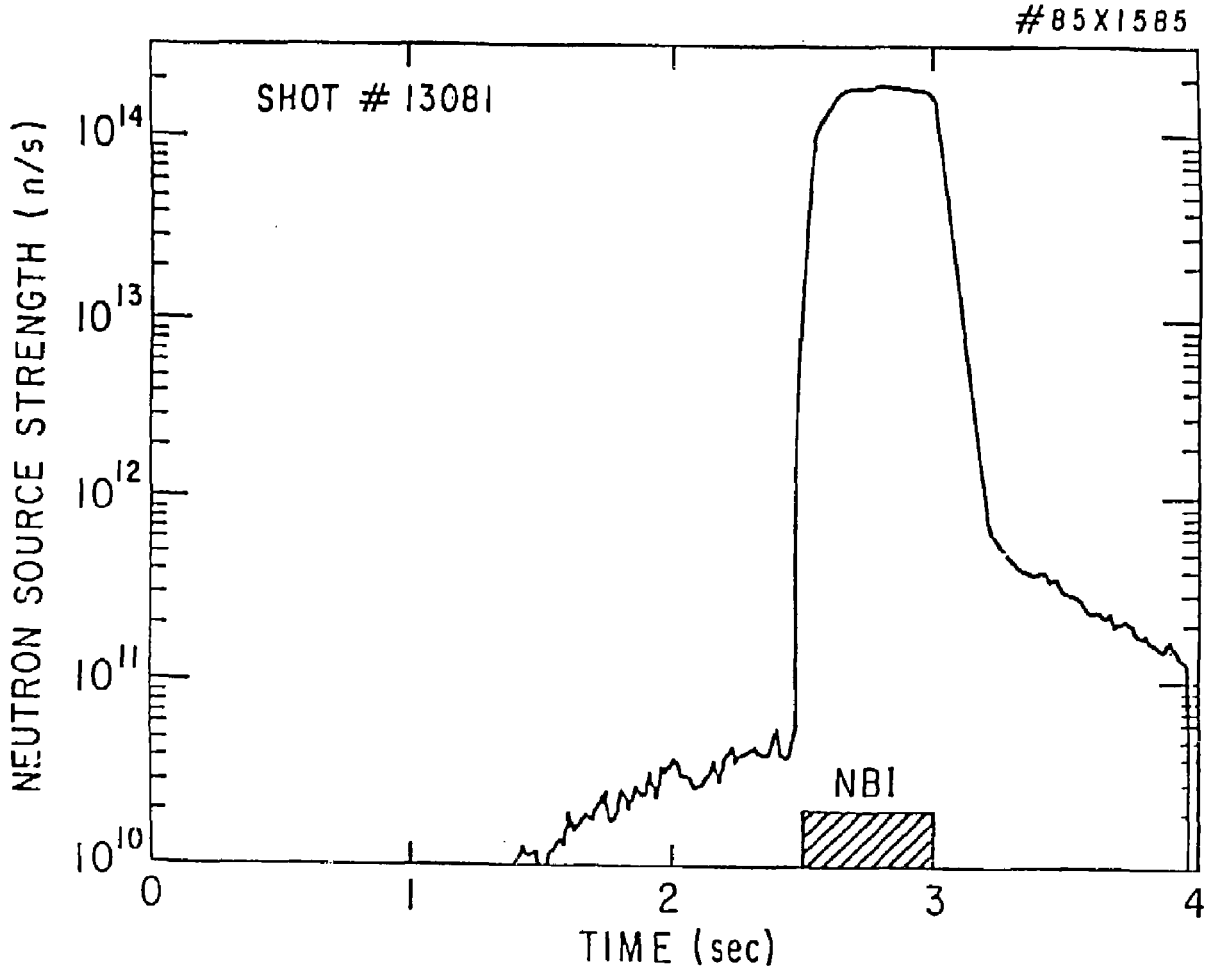
#85X1585
SHOT # 13081
NEUTRON SOURCE STRENGTH (n/s)
10^{14}
10^{13}
10^{12}
10^{11}
10^{10}
NBI
0
1
2
3
4
TIME (sec)

Fig. 2

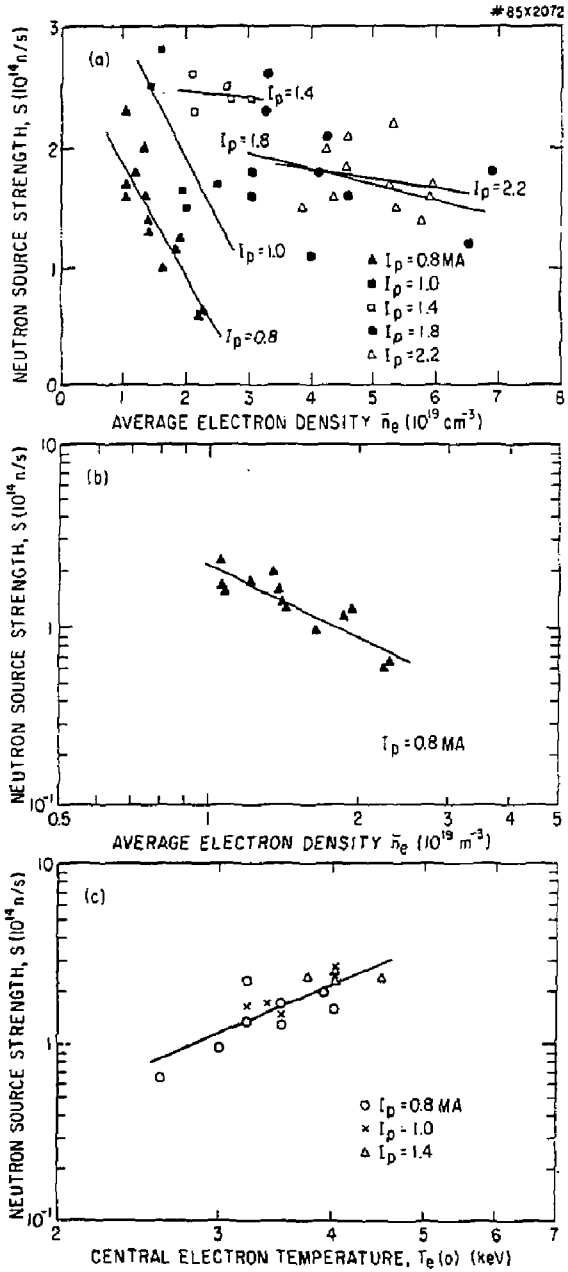
#85X2072
(a)
I_p=1.4
I_p=1.8
I_p=2.2
I_p=1.0
I_p=0.8
▲ I_p=0.8MA
■ I_p=1.0
□ I_p=1.4
● I_p=1.8
△ I_p=2.2
NEUTRON SOURCE STRENGTH, S (10^{14} n/s)
AVERAGE ELECTRON DENSITY $\bar{n}_e$ (10^{19} cm^{-3})
(b)
I_p=0.8 MA
NEUTRON SOURCE STRENGTH, S (10^{14} n/s)
AVERAGE ELECTRON DENSITY $\bar{n}_e$ (10^{19} m^{-3})
(c)
○ I_p=0.8 MA
× I_p=1.0
△ I_p=1.4
NEUTRON SOURCE STRENGTH, S (10^{14} n/s)
CENTRAL ELECTRON TEMPERATURE, T_e(o) (keV)

Fig. 3

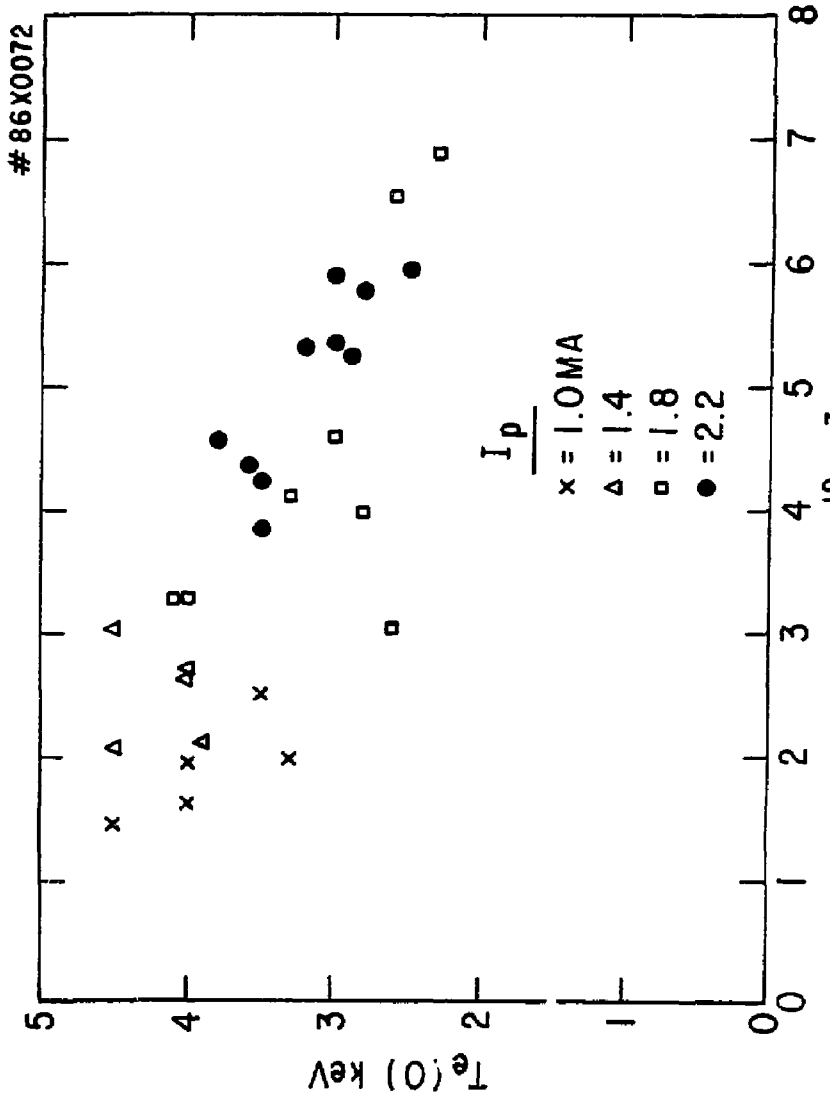

Fig. 4

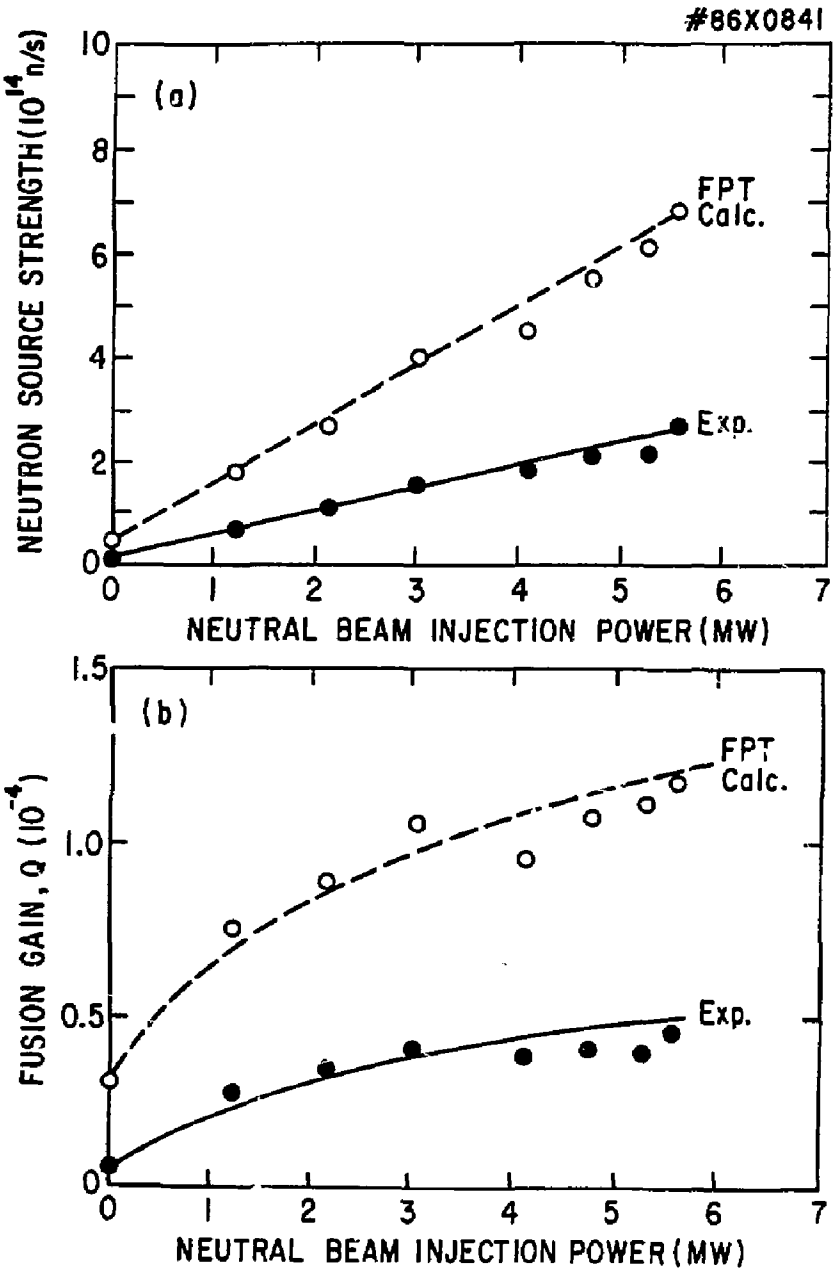
#86X0841
(a)
NEUTRON SOURCE STRENGTH (10^{14} n/s)
FPT Calc.
Exp.
NEUTRAL BEAM INJECTION POWER (MW)
(b)
FUSION GAIN, Q (10^{-4})
FPT Calc.
Exp.
NEUTRAL BEAM INJECTION POWER (MW)

Fig. 5

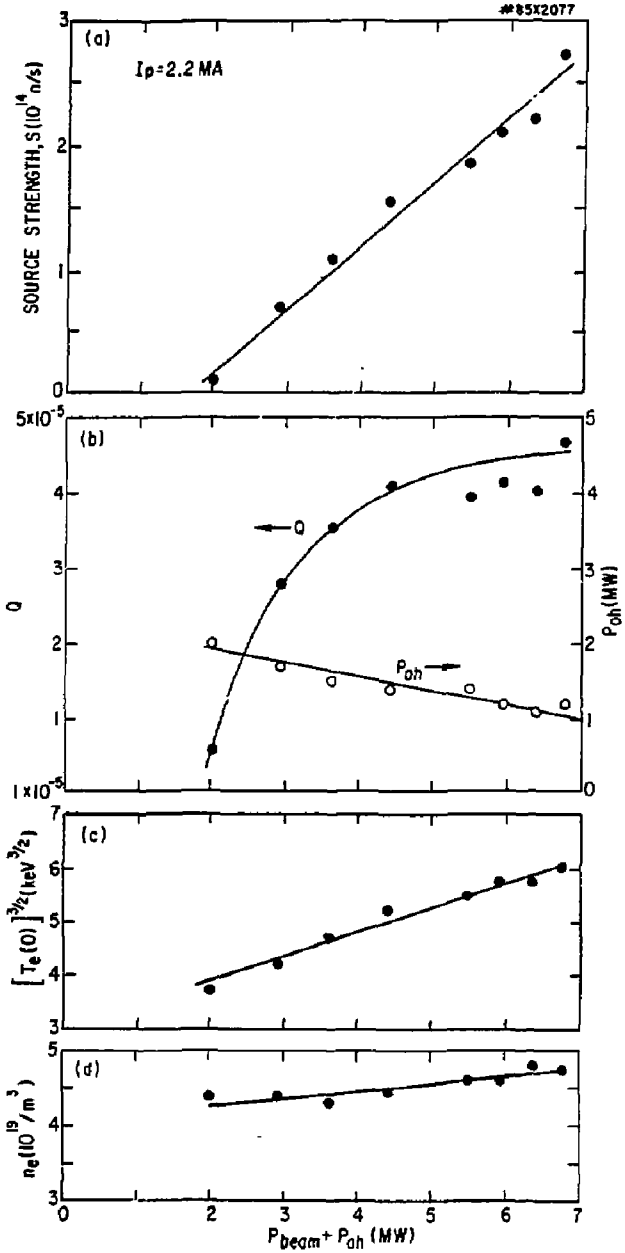
#85X2077
(a)
Ip=2.2 MA
SOURCE STRENGTH, S(10^14 n/s)
(b)
Q
P_oh
P_oh(MW)
(c)
[T_e(0)]^3/2 (keV^3/2)
(d)
n_e(10^19/m^3)
P_beam+P_oh (MW)

Fig. 6

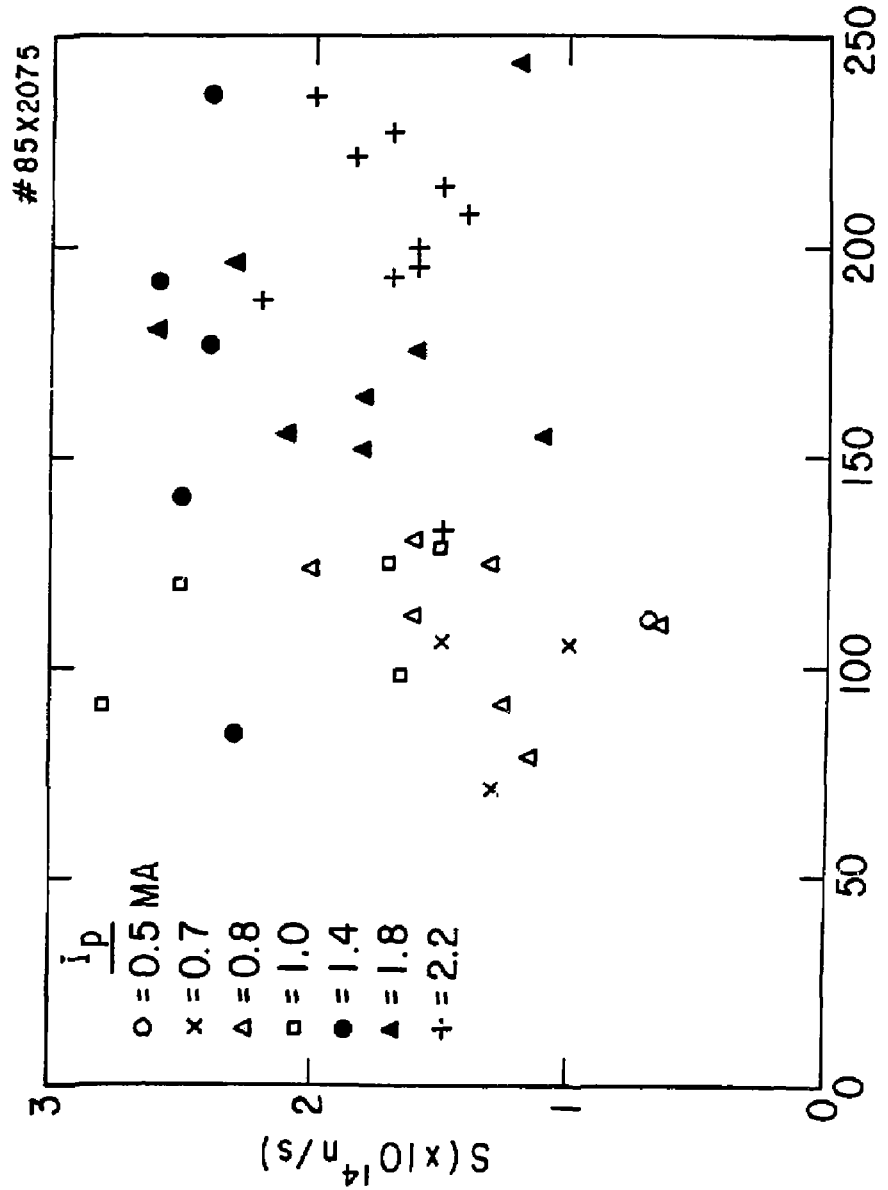
#85X2075
i_p
o = 0.5 MA
x = 0.7
Δ = 0.8
□ = 1.0
● = 1.4
▲ = 1.8
+ = 2.2
S (x10^{14}n/s)
τ_E (msec)
0
50
100
150
200
250
1
2
3

Fig. 7

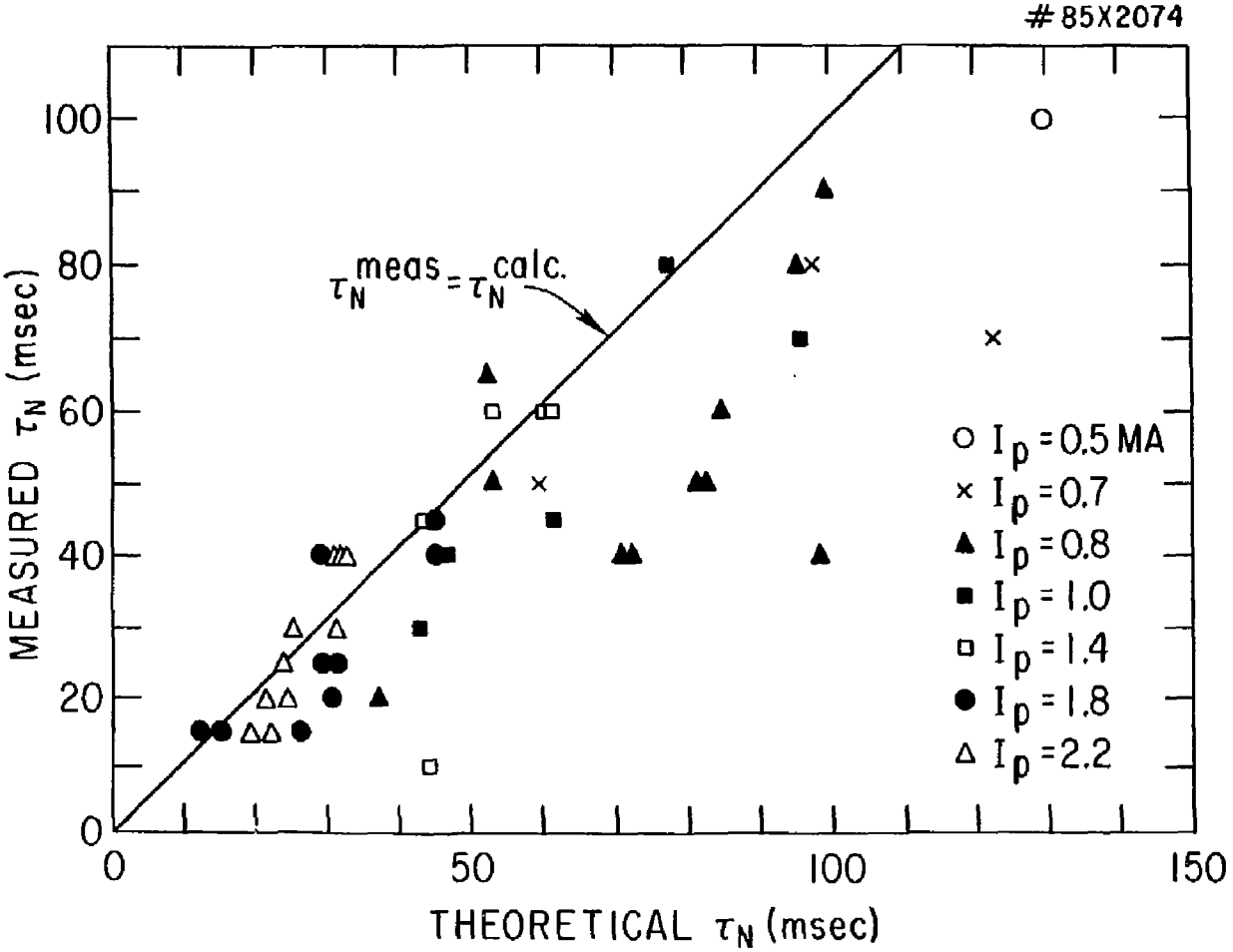
#85X2074
MEASURED τ_N (msec)
THEORETICAL τ_N (msec)
$\tau_N^{meas} = \tau_N^{calc.}$
I_p = 0.5 MA
I_p = 0.7
I_p = 0.8
I_p = 1.0
I_p = 1.4
I_p = 1.8
I_p = 2.2
0
20
40
60
80
100
0
50
100
150

Fig. 8

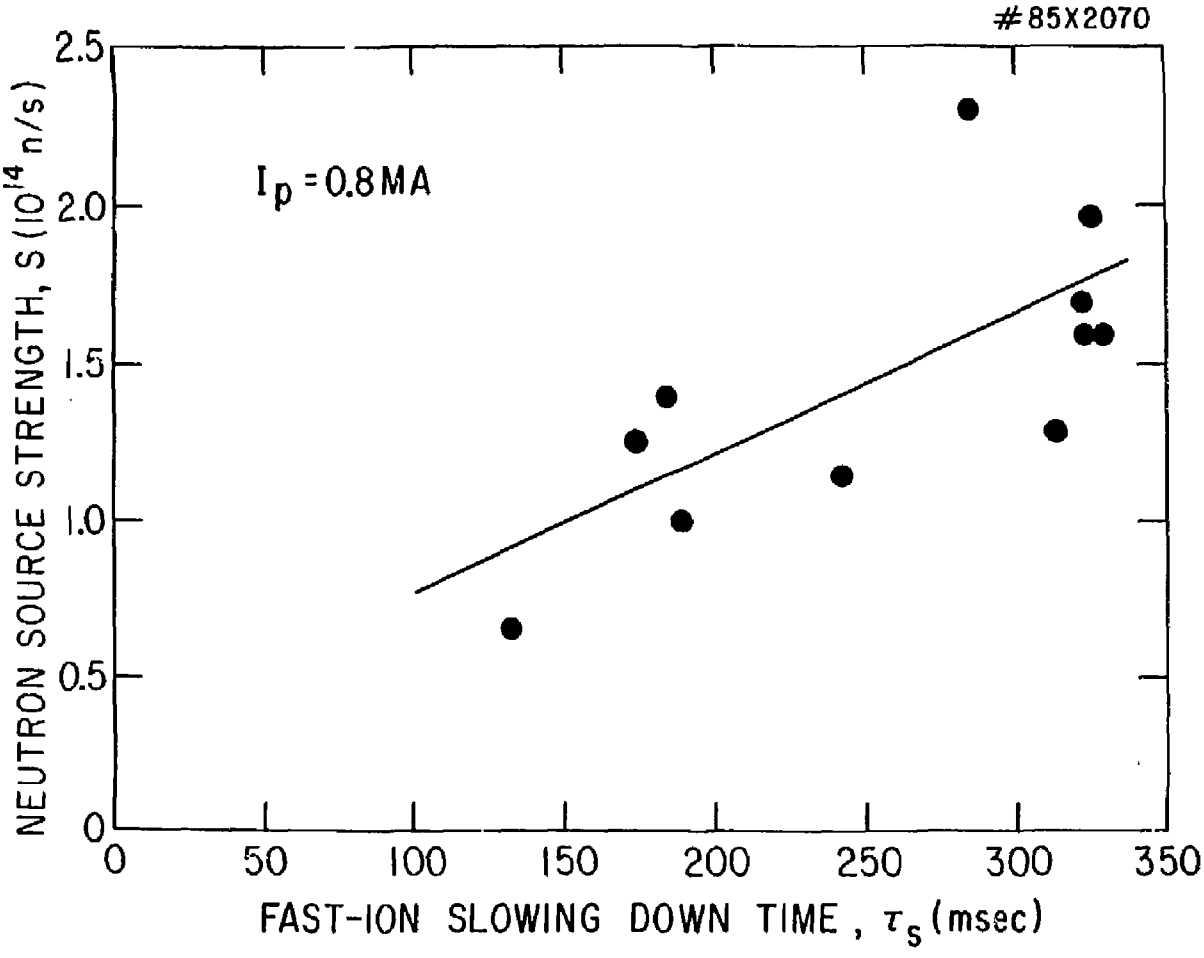
#85X2070
I_p = 0.8MA
NEUTRON SOURCE STRENGTH, S (10^{14} n/s)
2.5
2.0
1.5
1.0
0.5
0
0
50
100
150
200
250
300
350
FAST-ION SLOWING DOWN TIME, τ_s (msec)

Fig. 9

EXTERNAL DISTRIBUTION IN ADDITION TO UC-20

Plasma Res Lab, Austra Nat'l Univ, AUSTRALIA
Dr. Frank J. Paoloni, Univ of Wollongong, AUSTRALIA
Prof. I.R. Jones, Flinders Univ., AUSTRALIA
Prof. M.H. Brennan, Univ Sydney, AUSTRALIA
Prof. F. Cap, Inst Theo Phys, AUSTRIA
M. Goossens, Astronomisch Instituut, BELGIUM
Prof. R. Boucique, Laboratorium voor Natuurkunde, BELGIUM
Dr. D. Palumbo, Dg XII Fusion Prog, BELGIUM
Ecole Royale Militaire, Lab de Phys Plasmas, BELGIUM
Dr. P.H. Sakanaka, Univ Estadual, BRAZIL
Lib. & Doc. Div., Instituto de Pesquisas Espaciais, BRAZIL
Dr. C.R. James, Univ of Alberta, CANADA
Prof. J. Teichmann, Univ of Montreal, CANADA
Dr. H.M. Skarsgard, Univ of Saskatchewan, CANADA
Prof. S.R. Sreenivasan, University of Calgary, CANADA
Prof. Tudor W. Johnston, INRS-Energie, CANADA
Dr. Hannes Barnard, Univ British Columbia, CANADA
Dr. M.P. Bachynski, MPB Technologies, Inc., CANADA
Chalk River, Nucl Lab, CANADA
Zhengwu Li, SW Inst Physics, CHINA
Library, Tsing Hua University, CHINA
Librarian, Institute of Physics, CHINA
Inst Plasma Phys, Academia Sinica, CHINA
Dr. Peter Lukac, Komenskeho Univ, CZECHOSLOVAKIA
The Librarian, Culham Laboratory, ENGLAND
Prof. Schatzman, Observatoire de Nice, FRANCE
J. Radet, CEN-BP5, FRANCE
JET Reading Room, JET Joint Undertaking, ENGLAND
AM Dupas Library, AM Dupas Library, FRANCE
Dr. Tom Mual, Academy Bibliographic, HONG KONG
Preprint Library, Cent Res Inst Phys, HUNGARY
Dr. R.K. Chhajlani, Vikram Univ, INDIA
Dr. B. Dasgupta, Saha Inst, INDIA
Dr. P. Kaw, Physical Research Lab, INDIA
Dr. Phillip Rosenau, Israel Inst Tech, ISRAEL
Prof. S. Cuperman, Tel Aviv University, ISRAEL
Prof. G. Rostagni, Univ Di Padova, ITALY
Librarian, Int'l Ctr Theo Phys, ITALY
Miss Clelia De Palo, Assoc EURATOM-ENEA, ITALY
Biblioteca, del CNR EURATOM, ITALY
Dr. H. Yamato, Toshiba Res & Dev, JAPAN
Direc. Dept. Lg. Tokamak Dev. JAERI, JAPAN
Prof. Nobuyuki Inoue, University of Tokyo, JAPAN
Research Info Center, Nagoya University, JAPAN
Prof. Kyoji Nishikawa, Univ of Hiroshima, JAPAN
Prof. Sigeru Mori, JAERI, JAPAN
Prof. S. Tanaka, Kyoto University, JAPAN
Library, Kyoto University, JAPAN
Prof. Ichiro Kawakami, Nihon Univ, JAPAN
Prof. Satoshi Itoh, Kyushu University, JAPAN
Dr. D.I. Choi, Adv. Inst Sci & Tech, KOREA
Tech Info Division, KAERI, KOREA
Bibliotheek, Fom-Inst Voor Plasma, NETHERLANDS
Prof. B.S. Liley, University of Waikato, NEW ZEALAND
Prof. J.A.C. Cabral, Inst Superior Tecn, PORTUGAL
Dr. Octavian Petrus, ALI CUZA University, ROMANIA
Prof. M.A. Hellberg, University of Natal, SO AFRICA
Dr. Johan de Villiers, Plasma Physics, Nucor, SO AFRICA
Fusion Div. Library, JEN, SPAIN
Prof. Hans Wilhelmson, Chalmers Univ Tech, SWEDEN
Dr. Lennart Stenflo, University of UMEA, SWEDEN
Library, Royal Inst Tech, SWEDEN
Centre de Recherchesen, Ecole Polytech Fed, SWITZERLAND
Dr. V.T. Tolok, Kharkov Phys Tech Ins, USSR
Dr. D.D. Ryutov, Siberian Acad Sci, USSR
Dr. G.A. Eliseev, Kurchatov Institute, USSR
Dr. V.A. Glukhikh, Inst Electro-Physical, USSR
Institute Gen. Physics, USSR
Prof. T.J.M. Boyd, Univ College N Wales, WALES
Dr. K. Schindler, Ruhr Universitat, W. GERMANY
ASDEX Reading Rm, IPP/Max-Planck-Institut fur Plasmaphysik, F.R.G.
Nuclear Res Estab, Julich Ltd, W. GERMANY
Librarian, Max-Planck Institut, W. GERMANY
Bibliothek, Inst Plasmaforschung, W. GERMANY
Prof. R.K. Janev, Inst Phys, YUGOSLAVIA